Inorg. Chem. **2007**, *46*, 10926–10936

Theoretical Study of Metal–Ligand Interaction in Sm(III), Eu(III), and Tb(III) Complexes of Coumarin-3-Carboxylic Acid in the Gas Phase and Solution

Ivelina Georgieva,[†] Natasha Trendafilova,*[,†] Adélia J. A. Aquino,[‡] and Hans Lischka*[,‡]

Institute of General and Inorganic Chemistry, Bulgarian Academy of Sciences, Sofia, Bulgaria and Institute for Theoretical Chemistry, Währingerstrasse 17, University of Vienna, A-1090 Vienna, Austria

Received August 23, 2007

The interaction of lanthanide(III) cations (Ln(III) = Sm(III), Eu(III), and Tb(III)) with the deprotonated form of the coumarin-3-carboxylic acid (*cca*$^-$) has been investigated by density functional theory (DFT/B3LYP) and confirmed by reference MP2 and CCSD(T) computations. Solvent effects on the geometries and stabilities of the Ln(III) complexes were computed using a combination of water clusters and a continuum solvation model. The following two series of systems were considered: (i) Ln(*cca*)$^{2+}$, Ln(*cca*)$_2^+$, Ln(*cca*)$_3$ and (ii) Ln(*cca*)(H$_2$O)$_2$Cl$_2$, Ln(*cca*)$_2$(H$_2$O)$_2$Cl, Ln(*cca*)$_3$. The strength and character of the Ln(III)–*cca*$^-$ bidentate bonding were characterized by calculated Ln–O bond lengths, binding energies, ligand deformation energies, energy partitioning analysis, σ-donation contributions, and natural population analyses. The energy decomposition calculations predicted predominant electrostatic interaction terms to the Ln–*cca* bonding (ionic character) and showed variations of the orbital interaction term (covalent contributions) for the Ln–*cca* complexes studied. Electron distribution analysis suggested that the covalent contribution comes mainly from the interaction with the carboxylate moiety of *cca*$^-$.

Introduction

Recently, luminescent lanthanide complexes have attracted much attention because of their potential application to a wide range of processes and new technologies as luminescent materials (planar waveguide amplifiers, plastic lasers, and light-emitting diodes),[1−4] as fluoroimunoassays,[5,6] as antennas in photosensitive bioorganic compounds,[5,6] and for high technology optics. In spite of the great experimental research on luminescent lanthanide complexes, structure−property relationships are not yet clearly understood, and therefore, a basic concept for development and design of new luminescent lanthanide complexes is still missing.[7,8] Better understanding of the chemical properties of lanthanide luminescent complexes requires at first a precise description of their geometrical and electronic structures and the Ln−ligand bonding type. The Ln−ligand distances, energy levels, and ligand absorption bands obtained using different computational schemes appear as important characteristics for prediction of the ligand−lanthanide(III) energy-transfer rate and f−f transitions.[9−14] Detailed models for energy and charge

* To whom correspondence should be addressed. E-mail: hans.lischka@univie.ac.at, ntrend@svr.igic.bas.bg.
† Bulgarian Academy of Sciences.
‡ University of Vienna.

(1) Sabbatini, N.; Guardigli, M.; Lehn, J.-M. *Coord. Chem. Rev.* **1993**, *123*, 201.
(2) Steemers, F. J.; Verboom, W.; Reinhoudt, D. N.; van der Tol, E. B.; Verhoeven, J. W. *J. Am. Chem. Soc.* **1995**, *117*, 9408.
(3) Kang, T.-S.; Harrison, B. S.; Foley, T. J.; Knefely, A. S.; Boncelia, J. M.; Reynolds, J. R.; Schanze, K. S. *Adv. Mater* **2003**, *15*, 1093.
(4) Destri, S.; Porzio, W.; Meinardi, F.; Tubino, R.; Salerno, G. *Macromolecules* **2003**, *36*, 273.
(5) *Lanthanide probes in life, chemical, and earth sciences: Theory and practice*; Choppin, G. R., Bünzli, J.-C., Eds.; Elsevier: Amsterdam, 1989.
(6) Azevêdo, W. M de; dos Anjos, P. N. M.; Malta, O. L.; de Sá, G. F. *J. Lumin.* **1994**, *493*, 60.
(7) Kim, H. K.; Oh, J. B.; Baek, N. S.; Roh, S.-G.; Nah, M.-K.; Kim, Y. H. *Bull. Korean Chem. Soc.* **2005**, *26* (2), 201.
(8) Hemmila, I.; Laitala, V. *J. Fluoresc.* **2005**, *15* (4), 529.
(9) (a) de Andrare, A. V. M.; da Costa, N. B., Jr.; Simas, A. M.; de Sá, G. F. *Chem. Phys. Lett.* **1994**, *227*, 349. (b) de Sá, G. F.; Malta, O. L; de Mello Donega, C.; Simas, A. M.; Longo, R. L.; Santa-Cruz, P. A.; da Silva, E. F., Jr. *Coord. Chem. Rev.* **2000**, *196*, 165. (c) Faustino, W. M.; Malta, O. L.; de Sá, G. F. *J. Chem. Phys.* **2005**, *122*, 054109.
(10) Rocha, G. B.; Freire, R. O.; da Costa, N. B., Jr.; de Sá, G. F.; Simas, A. M. *Inorg. Chem.* **2004**, *43*, 2346.
(11) (a) Malta, O. *Chem. Phys. Lett.* **1982**, *87*, 27. (b) Albuquerque, R. Q.; Rocha, G. B.; Malta, O. L.; Porcher, P. *Chem. Phys. Lett.* **2000**, *331*, 519.
(12) Porcher, P.; Dos Santos, M. C.; Malta, O. *Phys. Chem. Chem. Phys.* **1999**, *1*, 397.

10.1021/ic7016616 CCC: $37.00
Published on Web 11/09/2007

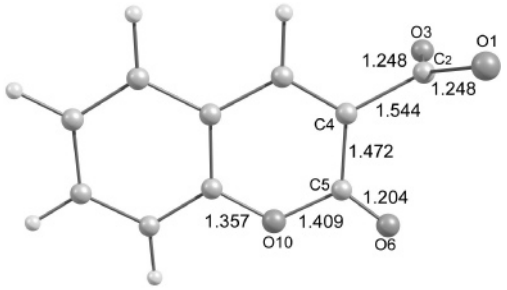

Figure 1. Optimized structure of cca^- in C_1 symmetry at the B3LYP/B1 level.

transfer have been developed in these investigations in terms of direct Coulomb, exchange, and charge-transfer effects and applied within semiempirical approaches. Various theoretical investigations have been carried out in order to rationalize the bonding of the lanthanide ions with σ N-donor ligands (neutral and anion)[15−17] and π-acceptor ligands (CO, $NCCH_3$).[15,18] However, there is still a lack of detailed structural information on the interaction of Ln(III) ions with bidentate σ O-donor ligands. Coumarin-3-carboxylic acid (*Hcca*) is an oxygen-donor ligand with efficient absorption properties. Its binding ability with respect to a series of lanthanide ions (La(III), Sm(III), Eu(III), Gd(III), Tb(III), Dy(III), and Er(III)) has been studied and discussed.[19−21] In complexation reactions, the active form of *Hcca* is the deprotonated one (cca^-), Figure 1. Bidentate bonding through the oxygen atom of the carbonylic group and the oxygen atom of the deprotonated carboxylic groups has been suggested for the Ln(III) complexes of cca^-[19,20] and confirmed by our previous calculations.[21]

Different photophysical properties of Ln(III)/cca^- complexes have been observed depending on the type of complex: Ln(*cca*)X_2·*n*solvent, Ln(*cca*)$_2$X·*n*solvent (Ln = Sm, Eu, Gd, Tb, Dy; X = Cl^-, ClO_4^-, NO_3^-; *n* is the number of solvent molecules),[19] and Eu(*cca*)$_3$·*n*solvent.[20] The luminescent behavior exhibits selectivity to the type of Ln(III) ion and the Ln:*cca* ratio (1:1, 1:2, 1:3). These spectroscopic investigations have revealed that the luminescence quantum yield of Sm(III), Tb(III), and Eu(III) complexes increases in that order. On the other side the luminescence quantum yield of Ln(III) increases with a decrease of the fluorescent quantum yield of the ligand when going from the 1:2 to the 1:1 complex.[19] In the 1:3 complex of Eu(III) the emission band only of the lanthanide ion was observed, indicating the most efficient energy-transfer process between the cca^- ligands and Eu(III) ion. The formation constants of Tb(III) complexes, evaluated in solution, have shown greater stability of the Tb(*cca*)$_2^+$ complex in relation to the Tb(*cca*)$^{2+}$ species.[19] The luminescence cation quantum yield of Tb(*cca*)$_2$(H_2O)Cl in solution is larger than that of Tb(*cca*)$_2$(H_2O)(NO_3), revealing an anionic effect.[19]

To gain deeper insight into the photophysical properties of the Ln(III) complexes of cca^- we undertook an extensive theoretical study of two series of Ln(III) complexes: (i) Ln(*cca*)$^{2+}$, Ln(*cca*)$_2^+$, and Ln(*cca*)$_3$ and (ii) Ln(*cca*)(H_2O)$_2Cl_2$, Ln(*cca*)$_2$(H_2O)$_2$Cl, and Ln(*cca*)$_3$ (Ln(III) = Sm(III), Eu(III), Tb(III)). The first series should provide the possibility of studying the properties of the isolated complexes, whereas the second series has been devised in order to model experimental situations in solution as realistically as possible. The purpose of this work is to investigate geometries, stabilities, and the nature and strength of the Ln(III)−*cca* bonding in the electronic ground state. The computed results for the series of Ln(III) complexes mentioned above are analyzed with respect to the (1) decreasing ionic radii in the order Sm(III), Eu(III), and Tb(III) (1.098, 1.087, and 1.063 Å, respectively), (2) number of cca^- ligands (Ln(III):*cca* = 1:1, 1:2, 1:3), and (3) type and number of counterions (Cl^-, NO_3^-). The anionic effect was studied on the basis of Tb(*cca*)$_2$(H_2O)Cl and Tb(*cca*)$_2$(H_2O)(NO_3) complex calculations. The Ln(III)−cca^- bonding situation and electron density distribution were investigated in terms of the natural population analysis (NPA), energy partitioning analysis (EPA), and charge decomposition analysis (CDA). To approach the experiment in solution, the Ln(III) complexes are further studied by a combination of an explicit water cluster approach (microsolvation) and an additional continuum solvation (global solvation) model. On the basis of these theoretical data we want to perform correlations with the above-mentioned luminescence properties in order to determine their relation with structural and chemical bonding properties.

Computational Details

DFT calculations were carried out using the Turbomole[22] and Gaussian03[23] programs. A combination of the basis sets developed in the group of Ahlrichs[24,25] was applied for the ligand atoms with the intention of finding a good compromise between efficiency and computational economy. The split-valence plus polarization (SV(P)) basis set was used (d polarization functions for the carbon, oxygen, chlorine, and nitrogen atoms, and an unpolarized SV basis for the hydrogen atoms).[24] In order to obtain a better description of the wave function in the ligand−Ln(III) interaction region, diffuse functions were added to the standard SV(P) basis set (one s and one p set) for the O atoms, for the C_2, C_4, and C_5 atoms included in the chelate ring (Figure 2), and for the Cl and N atoms. The exponents of the diffuse functions were obtained by dividing the respective smallest exponent of the SV(P) basis set by a factor of

(13) Zerner, M. C.; Loew, G. H.; Kirchner, R. F.; Mueller-Westerhoff, U. T. *J. Am. Chem. Soc.* **1980**, *102*, 589.
(14) de Andrade, A. V. M.; da Costa, N. B., Jr.; Longo, R. L.; Malta, O. L.; Simas, A. M. *Mol. Eng.* **1997**, *7*, 293.
(15) Vetere, V.; Maldivi, P.; Adamo, C. *J. Comput. Chem.* **2003**, *24*, 850.
(16) Gutierrez, F.; Rabbe, C.; Poteau, R.; Daudey, J. P. *J. Phys. Chem. A* **2005**, *109*, 4325.
(17) Maron, L.; Eisenstein, O. *J. Phys. Chem. A* **2000**, *104*, 7140.
(18) Tobish, S.; Nowak, Th.; Bögel, H. *J. Organomet. Chem.* **2001**, *619*, 24.
(19) Bisi Castellani, C.; Carugo, O. *Inorg. Chim. Acta* **1989**, *159*, 157.
(20) Roh, S.-G.; Baek, N. S.; Hong, K.-S.; Kim, H. K. *Bull. Korean Chem. Soc.* **2004**, *25* (3), 343.
(21) Mihaylov, Tz.; Trendafilova, N.; Kostova, I.; Georgieva, I.; Bauer, G. *Chem. Phys.* **2006**, *327*, 209.
(22) Ahlrichs, R.; Bär, M.; Häser, M.; Horn, H.; Kölmel, C. *Chem. Phys. Lett.* **1989**, *162*, 165.
(23) Gaussian98, 03, Revision C.02, references cited in www.gaussian.com.
(24) Schäfer, A.; Horn, H.; Ahlrichs, R. *J. Chem. Phys.* **1992**, *97*, 2571.
(25) Schäfer, A.; Huber, Ch.; Ahlrichs, R. *J. Chem. Phys.* **1994**, *100*, 5829.

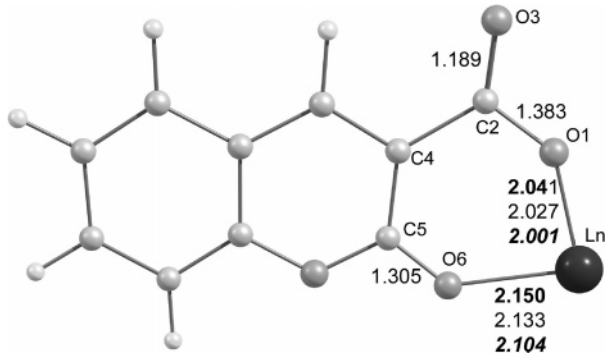

Figure 2. Optimized structures of the Ln(*cca*)$^{2+}$ complex, Ln(III) = Sm(III) (**bold**), Eu(III) (normal), Tb(III) (***italic***), at the B3LYP/B1 level.

3, as described in previous investigations.[26] These diffuse functions are important for the description of negatively charged regions of the complexes. Moreover, it was found previously that addition of these functions reduces the basis set superposition error significantly.[27] The combined basis set will be denoted as B1. SV(P)D denotes the basis set where diffuse functions on all heavy atoms had been added to the SV(P) basis.

Several DFT functionals were tested for the Eu(*cca*)$^{2+}$ complex using the B1 basis set: the nonhybrid PBE[28] and BLYP[29,30] functionals and the hybrid PBE0,[31,32] B3LYP,[29,33] and BHLYP[29,34] functionals. In order to confirm the density functional results, Møller−Plesset perturbation theory to second order (MP2)[35] geometry optimizations and single-point coupled-cluster calculations with singles and doubles substitutions plus a perturbative estimation of the triple excitations, CCSD(T),[36] have been performed at the B3LYP optimized geometry.

Theoretical investigations on a number of lanthanide(III) complexes have revealed that the 4f orbitals do not participate in the metal−ligand bond because of their contraction into the core.[17,18,37] Hence, for a structural description of complexes with 4f elements it is well acceptable to leave the 4f electrons in the core.[37−39] The main problem in the quantum mechanical treatment of lanthanides is the relativistic effects and degeneracy of the f orbitals. For heavy-metal complexes, the DFT formalism allows inclusion of part of the relativistic effects through two commonly used approaches: (i) use of a fully relativistic frozen core combined with a quasi-relativistic treatment of the valence shells via the zero-order regular approximation (ZORA)[40,41] or Pauli approaches[42] and (ii) use of relativistic effective core potentials (RECPs). As it is found in the literature, for the Ln(III) complexes with σ-donor ligands all relativistic DFT approaches provide consistent results, which are in very satisfying agreement with the experimental trends.[15] In line with the nonparticipation of the 4f electrons in the bonding, no effect of the spin−orbital (SO) coupling on the equilibrium geometries of Ln(III) complexes was found.[15] Therefore, the Ln(III) ions (La(III), Sm(III), Eu(III), and Tb(III)) were calculated in the DFT and CCSD(T) approaches using the relativistic effective core potential (RECP) optimized by the Stuttgart-Dresden group.[43−46] The large-core RECPs with 11 valence electrons in combination with their optimized valence basis sets (7s6p5d)/[5s4p3d] were used for the corresponding Ln(III) ions.[43] This ECP treats [Kr]4d^{10} (La), [Kr]4d^{10}4f^5 (Sm), [Kr]4d^{10}4f^6 (Eu), and [Kr]4d^{10}4f^8 (Tb) as fixed cores, and only the 5s^{2}5p^{6}6s^{2}5d^{1}6p^0 shell is taken into account explicitly.

Full geometry optimizations of all the molecular systems were carried out without symmetry constraint. Frequency calculations were performed, and the minima on the potential-energy surfaces of the reported structures were characterized by the absence of negative eigenvalues in the Hessian matrix. The electron density distribution of the Ln(III) complexes was characterized with the help of NPA.[47] In order to perform the NPA analysis with the Gaussian03 program a single f-type function on Sm ($\zeta = 0.2776$), Eu ($\zeta = 0.2859$), and Tb ($\zeta = 0.2866$) (ζ is the smallest exponent of the f-function set of the small ECP)[48] was added in this case.[18] Basis set superposition error (BSSE) corrections to the Ln(III)−*cca* binding energy were calculated for the B1 basis using the counterpoise method.[49,50] The bonding situation in the Ln−*cca* complexes was investigated by means of EPA and CDA.[51] The EPA is based on the methods of Morokuma[52] and Ziegler and Rauk[53] as implemented in the program package ADF(2005.01).[54] To overcome the problem with the open-shell f-valence orbitals, the partitioning scheme was performed at the PW91/TZP level[55] with B3LYP/B1-optimized structures of the La(III)−*cca* complexes. In these calculations the relativistic effects have been considered

(26) (a) Aquino, A. J. A.; Lischka, H.; Hättig C. *J. Phys. Chem. A* **2005**, *109*, 3201, (b) Georgieva, I.; Trendafilova, N.; Aquino, A. J. A.; Lischka, H. *J. Phys. Chem. A* **2005**, *109*, 11860.
(27) Aquino, A. J. A.; Tunega, D.; Haberhauer, G.; Gerzabek, M. H.; Lischka, H. *J. Phys. Chem. A* **2002**, *106*, 1862.
(28) Perdew, J. P. R.; Ernzerhof, M. *Phys. Rev. Lett.* **1996**, *77*, 3865.
(29) Lee, C.; Yang, W.; Parr, R. G. *Phys. Rev B* **1988**, *37*, 785.
(30) Lee, C.; Yang, W.; Parr, R. G. *Phys. Rev B* **1988**, *33*, 3098.
(31) Adamo, C.; Barone, V. *J. Chem. Phys.* **1999**, *110*, 6158.
(32) Perdew, J. P.; Ernzerhof, M. *J. Chem. Phys.* **1996**, *105*, 9982.
(33) Becke, A. D. *J. Chem. Phys.* **1993**, *98*, 5648.
(34) Becke, A. D. *J. Chem. Phys.* **1993**, *98*, 1372.
(35) Head-Gordon, M.; Head-Gordon, T. *Chem. Phys. Lett.* **1994**, *220*, 122.
(36) Pople, J. A.; Head-Gordon, M.; Raghavachari, K. *J. Chem. Phys.* **1987**, *87*, 5968.
(37) Boehme, C.; Coupez, B.; Wipff, G. *J. Phys. Chem. A* **2002**, *106*, 6487.
(38) Dobler, M.; Guilbaud, Ph.; Dedieu, A.; Wipff, G. *New. J. Chem.* **2001**, *25*, 1458.
(39) Maron, L.; Eisenstein, O. *New J. Chem.* **2001**, *25*, 255.
(40) Chang, C.; Pelissier, M.; Durand, P. *Phys. Scr.* **1986**, *34*, 394.
(41) (a) van Lenthe, E.; Baerends, E. J.; Snijders, J. G. *J. Chem. Phys* **1993**, *99*, 4597. (b) van Lenthe, E.; Baerends, E. J.; Snijders, J. G. *J. Chem. Phys.* **1994**, *101*, 9783. (c) van Lenthe, E.; Ehlers, A. E.; Baerends, E. J. *J. Chem. Phys.* **1999**, *110*, 8943.
(42) van Lenthe, E.; van Leeuwen, R.; Baerends, E. J.; Snijders, J. G. *Int. J. Quantum Chem.* **1996**, *57*, 281.
(43) Dolg, M.; Stoll, H.; Savin, A.; Preuss, H. *Theor. Chim. Acta* **1989**, *75*, 173.
(44) Dolg, M.; Fulde, P.; Kuechle, W.; Neumann, C.-S.; Stoll, H. *J. Chem. Phys.* **1991**, *94*, 3011.
(45) Dolg, M.; Stoll, H.; Preuss, H. *Theor. Chim. Acta* **1993**, *85*, 441.
(46) (a) Dolg, M.; Stoll, H. *Handbook on the Physics and Chemistry of Rare Earths;* Elsevier: Amsterdam, 1996; Vol. 22, Chapter 152. (b) Dolg, M.; Stoll, H. *Theor. Chim. Acta* **1989**, *75*, 369. (c) Dolg, M.; Stoll, H.; Preuss, H. *J. Chem. Phys.* **1989**, *90*, 1730. (d) Dolg, M.; Stoll, H.; Preuss, H. *J. Mol. Struct.* **1991**, *235*, 67. (e) Dolg, M.; Stoll, H.; Flad, H. T.; Preuss, H. *J. Chem. Phys.* **1992**, *97*, 1162. (f) Kaupp, M.; Schleyer, P. v. R.; Dolg, M.; Stoll, H. *J. Am. Chem. Soc.* **1992**, *114*, 8202.
(47) Reed, A. E.; Curtiss, L. A.; Weinhold, F. *Chem. Rev.* **1988**, *88*, 899.
(48) (a) Cao, X.; Dolg, M. *J. Chem. Phys.* **2001**, *115*, 7348. (b) Cao, X.; Dolg, M. *J. Mol. Struct. (THEOCHEM)* **2002**, *581*, 139.
(49) Xantheas, S. S. *J. Chem. Phys.* **1996**, *104* (21), 8821.
(50) (a) Boys, S. F.; Bernardi, F. *Mol. Phys.* **1970**, *19*, 553. (b) van Duijneveldt, F. B.; van Duijneveldt-van de Rijdt, J. G. C. M.; van Lenthe, J. H. *Chem. Rev.* **1994**, *94*, 1873. (c) Valiron, P.; Mayer, I. *Chem. Phys. Lett.* **1997**, *275*, 46.
(51) (a) Dapprich, S.; Frenking, G. *J. Phys. Chem.* **1995**, *99*, 93. (b) Frenking, G.; Pidun, U. *J. Chem. Soc., Dalton Trans.* **1997**, 1653. (c) The CDA calculations were carried out with the program CDA: Dapprich, S.; Frenking, G. *CDA*; Phillips-Universität: Marburg, 1994.
(52) Morokuma, K. *J. Chem. Phys.* **1971**, *55*, 1236.
(53) Ziegler, T.; Rauk, A. *Theor. Chim. Acta* **1977**, *46*, 1.
(54) te Velde, G.; Bickelhaupt, F. M.; Baerends, E. J.; Fonseca Guerra, C.; van Gisbergen, S. J. A.; Snijders, J. G.; Ziegler, T. *J. Comput. Chem.* **2001**, *22*, 931.
(55) Perdew, J. P.; Chevary, J. A.; Vosko, S. H.; Jackson, K. A.; Pederson, M. R.; Singh, D. J.; Fiolhais, C. *Phys. Rev. B* **1992**, *46*, 6671.

by means of ZORA.[40,41] Within this method, the binding energy between two fragments, ΔE_b, is split into the three components

$$\Delta E_b = \Delta E_{elstat} + \Delta E_{Pauli} + \Delta E_{orb}$$

ΔE_{elstat} gives the electrostatic interaction energy between the fragments, which is calculated with a frozen electron density distribution in the geometry of the complex. ΔE_{Pauli} represents the repulsive electron interactions between occupied orbitals, and ΔE_{orb} is the stabilizing orbital interaction due to the relaxation of the Kohn−Sham orbitals in the SCF procedure.

The CDA decomposes the Kohn−Sham determinant of a complex [ML] in terms of fragment orbitals of the chosen ligand L and the metal [M]. The [M] ← L donation is then given by mixing of the occupied orbitals of L and vacant orbitals of [M]. The [M] → L back-donation in return is given by the mixing of the occupied orbitals of [M] and vacant orbitals of L. The mixing of the occupied orbitals of both fragments gives the repulsive polarization (*r*), and the mixing of unoccupied orbitals gives the residual term (Δ) that should be small. The CDA calculations of the Ln(III) complexes were performed with the SV(P) basis set since the larger B1 basis gave large negative values for the residual term. A similar deterioration of the CDA results applying larger basis set was reported already in the literature.[56]

The solvent effect on the formation energy for the Ln(III)−*cca* complexes was computed on the basis of (1) water cluster models considering the specific solute−solvent interaction and (2) a combination of the water cluster approach and the conductor-like screening model (COSMO), where the solute molecule forms a cavity within the dielectric continuum of permittivity ϵ that represents the solvent.[57] The specific solvent interaction is modeled by means of water clusters, Ln(*cca*·H_2O)$(H_2O)_2Cl_2$, Ln(*cca*·H_2O)$_2$-$(H_2O)_2Cl$, and Ln(*cca*·H_2O)$_3$, where one solvent molecule of H_2O is hydrogen-bonded to the free carboxylic oxygen of cca^-.

Results and Discussion

Methodological Investigations on the Eu(*cca*)$^{2+}$ Complex. DFT methods have proven to be powerful and economic alternatives for calculations of sizable Ln complexes. Inspection of the literature, however, indicates that a correct theoretical modeling of the lanthanide compounds is still not a standard task, and good agreement obtained for one type of Ln complexes cannot be guaranteed for other types. Hence, it becomes of great importance to inspect the reliability of the computational methods employed. For the selection of suitable DFT levels of calculation, the Eu(*cca*)$^{2+}$ complex served as a benchmark example.

At all levels of calculation the Eu(*cca*)$^{2+}$ is a minimum energy structure in C_s symmetry, Figure 2. The Eu−O bond lengths and O−Eu−O bond angles obtained with various DFT functionals are given in Table 1, along with the reference geometries arising from MP2 optimization. The reliable determination of Ln−*cca* bond lengths is of great importance in relation to the $cca^- \rightarrow$ Ln(III) energy-transfer prediction. The DFT and MP2 optimizations showed differences up to 0.025 Å for Eu−O bond lengths and 1° for the O−Eu−O angles. As discussed in the literature, such a small influence of the theoretical methods on the structural parameters could be explained by the electrostatic character of the Ln(III)−ligand interaction.[15] The Eu−*cca* distances are sensitive to the amount of the Hartree−Fock exchange included in the functional. The Eu−O_1 and Eu−O_6 distances shorten by 0.012/0.021 and 0.014/0.021 Å, respectively, upon increasing the amount of the exact exchange in the functional (BLYP (0%), B3LYP (21%), and BHLYP (50%)), Table 1. A similar correlation of the Ln(II)−ligand and Cu(II)−ligand bonds along the amount of HF exchange in the density functionals was already reported in the literature.[58,59] The result above is in line with the molecular electrostatic potential (MEP) values on O_1(CO) and O_6(=C) of cca^-, which become more negative in the same order of functionals.[21] On the other hand, the increase of the natural charges of Eu(III) (2.62, 2.68, 2.75 *e*), O_1 (−1.09, −1.13, −1.18 *e*), and O_6 (−0.97, −1.01, −1.05 *e*) with an increase of the exact exchange in the functionals indicates increasing localization in the Eu(*cca*)$^{2+}$ complex. This effect further leads to a shortening of Eu−O bond lengths in the Eu(*cca*)$^{2+}$ complex in the order BLYP, B3LYP, and BHLYP (Table 1). A similar trend was also established for Cu(II) complexes of oxime analogues of glycine with covalent contribution to M−L bonding: upon increasing the exact exchange, the gas-phase basicity (GB) increased and M−L distances shortened.[60,61] There are systems, however, such as UI_3NCCH_3, where the M−L bond lengths become longer with an increase of the percentage of the exact exchange due to the complicated character of the M−L bonding − significant π-back-donation contributions, M → L charge transfer, etc.[15]

As can be seen from Table 1, the BLYP Eu−O bond lengths approach the MP2 ones best, followed by B3LYP ≅ PBE, BHLYP, and PBE0 values, which in this order slightly underestimate the Eu−O distances. The B3LYP calculations with SV(P) and SV(P)D basis sets showed a negligible difference of the computed Eu−O bond lengths, revealing an insignificant role of the diffuse functions for the Ln(III)−*cca* bond length description, Table 1. The last

Table 1. Geometry Parameters and Binding Energy (ΔE_b) of the Eu(*cca*)$^{2+}$ Complex Calculated at Different Levels of Theory (Bond Lengths in Å, Bond Angles in deg, Energies in kcal/mol)

	geometry[a]			
method	Eu−O_1	Eu−O_6	O_1EuO_6	ΔE_b[b]
PBE/B1	2.026	2.134	80.0	−624.1
BLYP/B1	2.039	2.147	80.0	−622.0
PBE0/B1	2.014	2.122	79.4	−618.6
B3LYP/SV(P)	2.023	2.130	79.8	−638.4
B3LYP/SV(P)D	2.027	2.132	79.5	−617.1
B3LYP/B1	2.027	2.133	79.5	−618.5
BHLYP/B1	2.018	2.126	78.8	−612.9
MP2(Full)[c]/B1	2.033	2.144	79.6	−593.7
CCSD(T)[d]/B1//MP2(Full)/B1	2.033	2.144	79.6	−610.7
CCSD(T)[d]/B1//B3LYP/B1	2.027	2.133	79.5	−611.8

[a] See atom numbering in Figure 2. [b] Binding energies without basis set superposition error correction. [c] Correlating all electrons. [d] Correlating valence electrons.

(56) Decker, S. A.; Klobukowski, M. *J. Am. Chem. Soc.* **1998**, *120*, 9342.
(57) Klamt, A.; Schüürmann, G. *J. Chem. Soc., Perkin Trans.* **1993**, *2*, 799.
(58) Poater, J.; Sola, M.; Rimola, A.; Rodriguez-Santiago, L.; Sodupe, M. *J. Phys. Chem. A* **2004**, *108*, 6072.
(59) Wang, D.; Zhao, C.; Phillips, D. L. *Organometallics* **2004**, *23*, 1953.
(60) Georgieva, I.; Trendafilova, N. *Chem. Phys.* **2006**, *321*, 311.
(61) Georgieva, I.; Trendafilova, N.; Rodriguez-Santiago, L.; Sodupe, M. *J. Phys. Chem. A* **2005**, *109*, 5668.

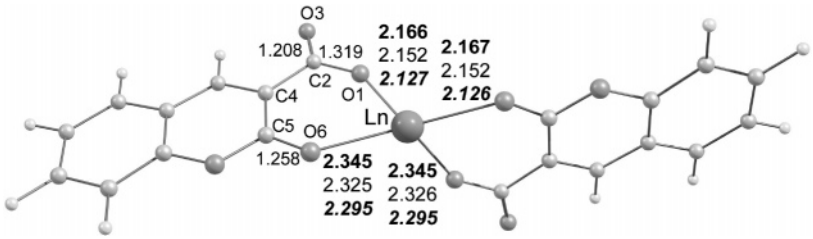

Figure 3. Optimized structures of the Ln(*cca*)$_2^+$ complex, Ln(III) = Sm(III) (**bold**), Eu(III) (normal), Tb(III) (***italic***), at the B3LYP/B1 level.

finding supports the interpretation of a dominant electrostatic character of the Ln(III)−*cca* bonds. Furthermore, the adequacy of the density functionals was checked with respect to the Eu(III)−*cca*$^-$ binding energy (ΔE_b) in comparison to the reference CCSD(T) calculation, Table 1. The effect of the geometry used (B3LYP or MP2) on the CCSD(T) binding energy is small since the results differ only by about 1 kcal/mol. The different functionals applied provided varying results for binding energies, indicating that the degree of charge and delocalization of the Ln(III) complexes are important. With an increase of the exact exchange (BLYP (PBE), B3LYP, BHLYP) the ΔE_b values approach the CCSD(T) result and the BHLYP binding energy is in best agreement with the CCSD(T) value. Table 1 also shows the importance of the diffuse functions added to the SV(P) basis for the B3LYP case. From SV(P) to SV(P)D the reduction of the binding energy (in absolute value) is 20 kcal/mol (∼3%). The difference between the SV(P)D and B1 values of ΔE_b is small (about 1 kcal/mol), which shows that it is sufficient to include the diffuse functions in the bonding region.

Our methodological investigations indicated that the B3LYP functional is a good compromise for geometry and binding energy calculations of the Eu(*cca*)$^{2+}$ complex. To check the B3LYP ability for description of the lanthanide contraction in the case of bidentate binding of *cca*$^-$, we calculated the La(*cca*)$^{2+}$ and Lu(*cca*)$^{2+}$ structures at the MP2 and B3LYP levels. The experimental value of 0.179 Å of lanthanide contraction[62] is very well reproduced in the case of *cca*$^-$ ligand ($\Delta_{lanthanide} = R_e(La(cca)^{2+}) - R_e(Lu(cca)^{2+})$ by the MP2 method − 0.181 Å for Ln−O_1 and 0.211 Å for Ln−O_6. The B3LYP values obtained for the bond differences above are slightly larger, 0.199 and 0.222 Å, respectively. The deviations obtained could be derived from the complex character of the Ln(III)−O binding in the six-membered ring where steric factors are also operative.

On the basis of the present density functional tests and experience gained in other previous studies on Ln(III) complexes with σ-donor ligands,[17,38,39,63] we chose the B3LYP functional together with the B1 basis set for our further calculations of the Ln(III)−*cca*$^-$ complexes. Our recent theoretical investigations on coumarin-3-carboxylic acid have also shown that B3LYP is a good compromise for calculations of geometry parameters and vibrational frequencies.[21]

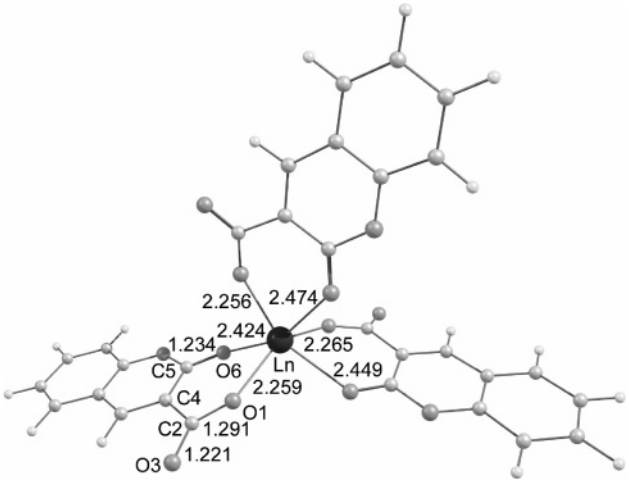

Figure 4. Optimized structure of the Ln(*cca*)$_3$ complex at the B3LYP/B1 level (Ln = Eu).

Optimized Geometries of Ln(III)−*cca*$^-$ Complexes. The Ln(III)−*cca*$^-$ complexes are studied in two series: series A, Ln(*cca*)$^{2+}$, Ln(*cca*)$_2^+$, and Ln(*cca*)$_3$, and series B, Ln(*cca*)$(H_2O)_2Cl_2$, Ln(*cca*)$_2(H_2O)_2$Cl, and Ln(*cca*)$_3$ (Ln(III) = Sm(III), Eu(III), and Tb(III)). The complexes of the first series contain only *cca* ligands. They have been chosen in order to reveal the properties of the isolated complexes in relation to the number of *cca*$^-$ molecules, whereas the second series has been derived from experimentally observed compositions of these complexes.[19,20] The Ln(*cca*)$_3$ calculations are performed mainly for Eu(III) since experimental data are available.[20] Selected geometry data of *cca*$^-$ and its Ln(III) complexes are given in Figures 1−6. Complete geometries in Cartesian coordinates can be found in the Supporting Information. The main focus of our discussion will be on the Ln−O_1/O_6(*cca*$^-$), Ln−H_2O, and Ln−X$^-$ (X$^-$ = Cl$^-$, NO_3^-) distances as indicators of Ln−ligand bonding strengths.

Series A. The B3LYP/B1-optimized geometries of the first series of structures are shown in Figures 2−4. The calculated Ln(*cca*)$^{2+}$ complexes are minima in C_s symmetry. The Ln(*cca*)$_2^+$ structures showed two minima: one in C_s (trans position) and one in C_1 symmetry with a dihedral angle C_5O_6-$LnO_{6'} \approx 136°$. The latter structure is energetically preferred by 10.9 kcal/mol. The Ln(*cca*)$_3$ structure has been optimized only for Eu(III) and shows one minimum in C_1 symmetry. Since the analysis of the calculated Ln(III)−O bond lengths revealed the same trends in all complexes studied we discuss only the Eu(III)−*cca*$^-$ complexes in detail. The shortest Eu−O distances are calculated for the Eu(*cca*)$^{2+}$ structure.

(62) (a) Shannon, R. D.; Prewitt, C. T. *Acta Crystallogr., Sect. B* **1969**, *25*, 925. (b) David, F.; Samhoun, K.; Guillaumont, R.; Edelstein, N. *J. Inorg. Nucl. Chem.* **1978**, *40*, 69.
(63) Boehme, C.; Wipff, G. *Inorg. Chem.* **2002**, *41* (4), 727.

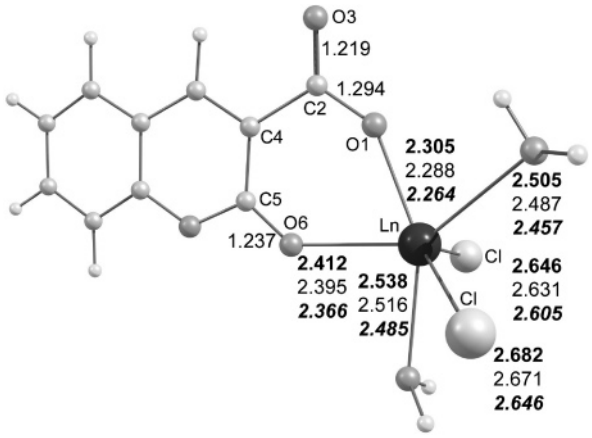

Figure 5. Optimized structures of Ln(*cca*)$(H_2O)_2Cl_2$, Ln(III) = Sm(III) (**bold**), Eu(III) (normal), Tb(III) (***italic***), at the B3LYP/B1 level.

With an increase of the number of cca^- ligands the Eu−O_1/O_6 bond lengths increase by 0.13/0.19 Å in Eu$(cca)_2^+$ and 0.23/0.32 Å in Eu$(cca)_3$. The elongation is larger for the weaker Eu−O_6 bond as compared to the stronger Eu−O_1 bond.

Series B. The Ln(*cca*)$(H_2O)_2Cl_2$ and Ln$(cca)_2(H_2O)_2$Cl structures were optimized using different input geometries with various locations of the Cl and H_2O ligands around the central Ln(III). The B3LYP/B1 optimizations always led to one and the same minimum structure in each case. The resulting structures are shown in Figures 5 and 6. Some calculated bond lengths of Eu−*cca* complexes are given in Table 2, and for complexes with two and three cca^- ligands, the average bond length is presented. The relation between the Eu−*cca* distances and the number of cca^- ligands in the complexes of series B is more complicated than that obtained for series A due to the presence of Cl^- counterions and H_2O molecules. For comparison, the Eu$(cca)_3$ structure is also included in the discussion on the neutral Ln(III) complexes. The shortest Eu−O_1(CO) distances are calculated for Eu$(cca)_3$, whereas the shortest Eu−O_6(=C) distance is found for the Eu(*cca*)$(H_2O)_2Cl_2$ complex, Table 2. In the Eu(III) complexes the Eu−O_w distances are always longer than the Eu−O_{cca} ones. The longest bond lengths are observed for the Eu−Cl bond. The shorter Eu−O_w and Eu−Cl bond lengths in Eu(*cca*)$(H_2O)_2Cl_2$ as compared to those in Eu$(cca)_2(H_2O)_2$Cl indicate stronger Eu−H_2O and Eu−Cl interactions in the former complex.

To estimate the effect of the anion (Cl^-, NO_3^-) on the structure and energetics of Ln(III)−cca^- complexes, modeling of Tb$(cca)_2(H_2O)$Cl and Tb$(cca)_2(H_2O)(NO_3)$ complexes was performed. The comparison of the structures of the two complexes shows similar Tb−O_1 bond lengths and a slightly shorter Tb−O_6 bond length for the first complex, Table 2. The NO_3^- group in Tb$(cca)_2(H_2O)(NO_3)$ is bonded to Tb(III) in a bidentate manner. Geometry optimizations starting with a monodentate Tb−ONO_2 structure led also to bidentate O_2NO binding. The X-ray structure of the La$(NO_3)_3(H_2O)_6$ complex has revealed a bidentate binding of NO_3^- groups to La(III) ion as well.[64]

The solvent effect on the Eu−O bond lengths derived from geometry optimizations of the Eu$(cca)^{2+}$, Eu(*cca*)$(H_2O)_2Cl_2$, Eu$(cca)_2(H_2O)_2$Cl, and Eu$(cca)_3$ complexes is summarized in Table 2. The calculated Ln(III)−ligand bond lengths in solution should give information on the bonding strength of the Ln(III) complexes in a real experimental situation. Upon inclusion of the solvent environment elongation of the Eu−O_1 and Eu−O_6 bond lengths by ∼0.25 Å is observed for the Eu$(cca)^{2+}$ model complex. Much smaller solvent effects are found for the Eu(*cca*)$(H_2O)_2Cl_2$, Eu$(cca)_2(H_2O)_2$Cl, and Eu$(cca)_3$ complexes since the first coordination shell of the Eu(III) cation has already been saturated and the global environment effects represent only the influence of outer solvation spheres. In solution, the Eu−O_6 bond lengths of Eu(*cca*)$(H_2O)_2Cl_2$, Eu$(cca)_2(H_2O)_2$Cl, and Eu$(cca)_3$ complexes shorten by ∼0.019 Å (average value) with respect to the isolated cluster. At the same time, the Eu−O_1 distance remains unchanged in Eu(*cca*)$(H_2O)_2Cl_2$, whereas it elongates in the Eu$(cca)_2(H_2O)_2$Cl and Eu$(cca)_3$ complexes. As a result, in solution both Eu−O_1/O_6 distances are the shortest ones (the strongest Eu(III)−*cca* interaction) in Eu(*cca*)$(H_2O)_2Cl_2$ followed by those of Eu$(cca)_3$ and Eu$(cca)_2(H_2O)_2$Cl. Shorter Eu−O_w and Eu−Cl bond lengths in solution are also found for Eu(*cca*)$(H_2O)_2Cl_2$ as compared to Eu$(cca)_2(H_2O)_2$Cl (the same trend as in the gas phase).

A survey of the structural data obtained helps to draw the following common trends. In all complexes studied the Ln−O_1 and Ln−O_6 distances become shorter with a decrease of the Ln(III) ionic radii in the order Sm(III), Eu(III), and Tb(III). In the complexes with a Ln:*cca* ratio of 1:1, the Ln−O_1(CO) distance is shorter by ∼0.1 Å than Ln−O_6(=C), while in the complexes with ratios Ln:*cca* = 1:2 and Ln:*cca* = 1:3, the bond length difference increases up to 0.2 Å. It should be noted that this difference between Ln−O_1(CO) and Ln−O_6(=C) distances is approximately the same in case of the bare Ln−*cca* complexes and the ones including counterions even though the absolute values of these distances strongly depend on the case. The gas phase as well as global solvation calculations predict a slightly shorter Eu−O_1 bond length in Eu(*cca*)$(H_2O)_2Cl_2$ than that in Eu$(cca)_2(H_2O)_2$Cl. The shortest Eu−O_1 bond length in the gas phase is found for the Eu$(cca)_3$ complex, whereas in solution the shortest Eu−O_1 bond length is obtained for the Eu(*cca*)$(H_2O)_2Cl_2$ complex. However, it has to be noted that the difference in the Eu−O_1 bond lengths, especially between Eu$(cca)_2(H_2O)_2$Cl and Eu$(cca)_3$, is extremely small.

CCA Deformation Energy. Upon binding to Ln(III), the cca^- ligands distort in order to minimize the interligand repulsion. The Ln(III)−*cca* bonding interactions are analyzed in terms of deformation of the cca^- ligands. The comparison between the bond lengths of the isolated cca^- (Figure 1) and the ones in the complexes (Figures 2−6) shows the greatest changes for the $C_{2-}O_1$ and C_5=O_6 bonds. Generally,

(64) Eriksson, B.; Larson, L. O.; Niinistö, L.; Valkonen, J. *Inorg. Chem.* **1980**, *19*, 1207.

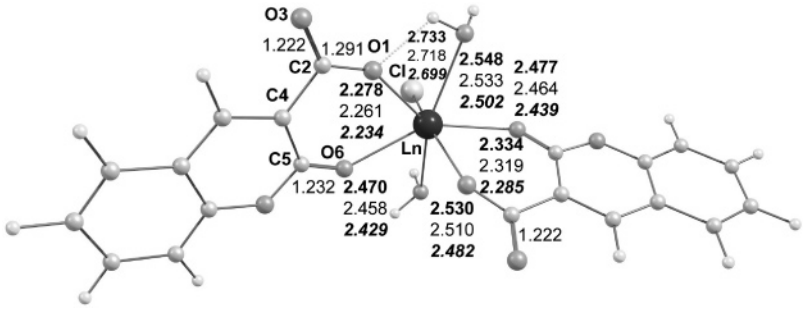

Figure 6. Optimized structures of Ln(*cca*)$_2$(H$_2$O)$_2$Cl, Ln(III) = Sm(III) (**bold**), Eu(III) (normal), Tb(III) (***italic***), at the B3LYP/B1 level.

Table 2. Geometry Parameters of Eu(III) and Tb(III) Complexes with *cca*$^-$ Calculated at the B3LYP/B1 Level in the Gas Phase and Solution (COSMO Continuum Model) (Bond Lengths, *R*, in Å)

	R(Ln−O$_1$)		*R*(Ln−O$_6$)		*R*(Ln−O$_w$)		*R*(Ln−Cl)		*R*(Ln−O$_{NO3}$)
system	gas	sol	gas	sol	gas	sol	gas	sol	gas
Eu(*cca*)$^{2+}$	2.027	2.276	2.133	2.373					
Eu(cca)$_2^+$	2.152^{av}		2.326^{av}						
Eu(*cca*)(H$_2$O)$_2$Cl$_2$	2.288	2.282	2.395	2.377	2.502^{av,a}	2.431^{av}	2.651^{av}	2.711^{av}	
Eu(*cca*)$_2$(H$_2$O)$_2$Cl	2.290^{av}	2.312^{av}	2.461^{av}	2.437^{av}	2.522^{av}	2.472^{av}	2.718	2.761	
Eu(*cca*)$_3$	2.260^{av}	2.305^{av}	2.449^{av}	2.433^{av}					
Tb(*cca*)$_2$(H$_2$O)Cl	2.224^{av}		2.394^{av}		2.476		2.649		
Tb(*cca*)$_2$(H$_2$O)NO$_3$	2.220^{av}		2.419^{av}		2.504				2.479^{av}

^{a} av = average value of bond lengths.

in Ln(*cca*)$^{2+}$ and Ln(*cca*)$_2^+$ the C−O bond elongations depend slightly on the Ln(III) type. The largest effects are found for the Tb(III) complexes. For the complexes of series B, the C−O bond elongations are less dependent on the Ln-(III) type. The ligand bond lengths displayed in Figures 2−6 are given for the Eu(III) complexes. Large C−O elongations were calculated for the isolated Ln(*cca*)$^{2+}$ species (with values of 0.10−0.14 Å), whereas in Ln(*cca*)(H$_2$O)$_2$Cl$_2$ and Ln(*cca*)$_2$(H$_2$O)$_2$Cl complexes the C−O bond lengths increase only by 0.03−0.05 Å. The calculated deformation energies, summarized in Table 3 (third column), give a comprehensive characterization of the ligand distortions. For the Ln(III) complexes containing more than one *cca*$^-$ ligand only the average deformation energies are presented. With an increase of the number of *cca*$^-$ ligands, in both series of structures Eu(*cca*)$^{2+}$, Eu(*cca*)$_2^+$, and Eu(*cca*)$_3$ and Eu(*cca*)(H$_2$O)$_2$Cl$_2$, Eu(*cca*)$_2$(H$_2$O)$_2$Cl, and Eu(*cca*)$_3$, the *cca*$^-$ deformation energies decrease, indicating a decrease of the Eu−*cca* interaction strength per ligand. For the complexes of series A, the decreasing ligand deformation energies correlate with the increasing Eu−O distances. For the complexes of series B, the ligand deformation energy is calculated between 8.1 and 9.4 kcal/mol. However, the correlation with the Eu−O distances is not so clear due to the more complicated pattern of Eu−O distance changes produced from the Cl$^-$ and H$_2$O binding to Eu(III). The *cca* deformation energies calculated for the Ln(III) complexes of both series is mainly due to the induced polarization of the ligand upon interaction with the Ln(III) cation. The bond length variations of *cca*$^-$ upon interaction with La(III) were explained previously in terms of the NBO analysis.[21] When the direction of the induced bond orbital polarization (BOP) coincided with the basic, unperturbed one of *cca*$^-$, the resultant bond orbital polarization increased and the covalent contribution decreased, causing an elongation of the bond length. Conversely, when the induced bond orbital polarization was opposite to the basic one of *cca*$^-$, the resultant BOP decreased, the covalent contribution increased, and the bond length shortened. Knowledge of the nature of the Ln(III)−*cca*$^-$ binding as well as the direction and extent of the *cca*$^-$ deformation are useful

Table 3. Binding Energies Ln(III)−*cca*$^-$ (ΔE_b, in kcal/mol), BSSE Corrected, Deformation Energies of *cca*$^-$ (ΔE_{def} in kcal/mol), and Formation Energies (ΔE_f, in kcal/mol) of the Ln(III) Complexes at the DFT/B3LYP/B1 Level

			ΔE_f		
systems	ΔE_b ^{BSSE}	ΔE_{def}^{a}	clust.	clust. + sol.	reaction no.^{b}
		class A			
Sm(*cca*)$^{2+}$	−611.6	33.6	−294.7	−23.1	2
Sm(*cca*)$_2^+$	−305.3^{av,c}	14.8^{av}	−482.9	−49.0	3
Eu(*cca*)$^{2+}$	−617.4	34.3	−295.3	−25.1	2
Eu(*cca*)$_2^+$	−307.6^{av}	14.6^{av}	−484.3	−50.8	3
Tb(*cca*)$^{2+}$	−628.1	34.8	−297.0	−24.7	2
Tb(*cca*)$_2^+$	−312.4^{av}	14.9^{av}	−486.5	−51.1	3
		class B			
Sm(*cca*)(H$_2$O)$_2$Cl2	−197.9	9.3	−551.0	−57.6	4
Sm(*cca*)$_2$(H$_2$O)$_2$Cl	−172.3^{av}	8.1^{av}	−559.4	−61.0	5
Sm(*cca*)$_3$			−568.6	−60.5	6
Eu(*cca*)(H$_2$O)$_2$Cl$_2$	−199.2^d	9.4	−551.5	−58.6	4
Eu(*cca*)$_2$(H$_2$O)$_2$Cl	−173.4^{av,e}	8.2^{av}	−560.5	−63.0	5
Eu(*cca*)$_3$	−167.1^{av,f}	8.1^{av}	−570.0	−62.5	6
Tb(*cca*)(H$_2$O)$_2$Cl$_2$	−201.8	9.4	−553.2	−58.6	4
Tb(*cca*)$_2$(H$_2$O)$_2$Cl	−173.8^{av}	8.3^{av}	−562.3	−63.4	5
Tb(*cca*)$_2$(H$_2$O)Cl	−180.5^{av}	8.6^{av}	−558.6	−58.7	7
Tb(*cca*)$_2$(H$_2$O)NO$_3$	−180.7^{av}	8.6^{av}	−580.0	−70.1	8
Tb(*cca*)$_3$			−572.5	−62.9	6

^{a} Energy difference of the *cca*$^-$ in the complex and the isolated *cca*$^-$. ^{b} For definition of reactions, see the text. ^{c} av = average value of E_b. ^{d} ΔE_b(Eu(H$_2$O)$_2$Cl$_2$-*cca*) = E(Eu(*cca*)(H$_2$O)$_2$Cl$_2$) − E(Eu(H$_2$O)$_2$Cl$_2$)$^+$ − E(*cca*$^-$). ^{e} ΔE_b(Eu(*cca*)(H$_2$O)$_2$Cl-*cca*) = E(Eu(*cca*)$_2$(H$_2$O)$_2$Cl) − E(Eu(*cca*)(H$_2$O)$_2$Cl)$^+$ − E(*cca*$^-$). ^{f} ΔE_b(Eu(*cca*)$_2$-*cca*) = E(Eu(*cca*)$_3$) − E(Eu(*cca*)$_2^+$) − E(*cca*$^-$).

for determination of the changes in the electron density distribution in the Ln(III)−*cca*$^-$ complexes studied.

Ln(III)−*cca* Binding Energies. For all Ln(III)−*cca* complexes, the Ln(III)−*cca*$^-$ binding energy per ligand was calculated according to the equation

$$\Delta E_b = E_{complex} - E(cca^-) - E(LnX^+) \quad (1)$$

where $E(cca^-)$ and $E(LnX^+)$ are the energies of *cca*$^-$ and the rest fragment LnX^+, respectively, at the complex geometry. The binding energies corrected for BSSE are collected in Table 3. The BSSE corrections for Ln−*cca* bonding vary between 1.0 and 4.4 kcal/mol. For the structures of series A, the Ln(III)−*cca* binding energy decreases in absolute value with increasing number of ligands which is in keeping with the increasing Ln−O bond lengths and decreasing ligand deformation energies.

For the complexes of series B, the presence of Cl^- and H_2O does not alter the ordering found for the complexes of series A. The absolute value of ΔE_b per ligand decreases in the series Ln(*cca*)$(H_2O)_2Cl_2$ > Ln(*cca*)$_2(H_2O)_2Cl$ > Ln(*cca*)$_3$. The ordering of the calculated binding energies is in agreement with the *cca*$^-$ deformation energies, indicating that binding strength decreases in the order above. The survey of ΔE_b values for 1:2 Tb−*cca* complexes reveals that the number of H_2O molecules and type of anionic ligand (Cl^- and NO_3^-) do not change the trend found above, Table 3. The same Tb−*cca* binding energies were obtained for Tb(*cca*)$_2(H_2O)Cl$ and Tb(*cca*)$_2(H_2O)(NO_3)$ complexes, showing no anionic effect on the Tb−*cca* bonding strength.

In agreement with the decreasing Ln(III) ionic radii in the order Sm(III) > Eu(III) > Tb(III), the Ln(III)−*cca*$^-$ bonding strength becomes stronger in that order for a given type of complex.

Formation Energies. The formation energies (ΔE_f) of the Ln(III) complexes are defined by the following reactions where the solvated Ln(III) cation reacts with solvated *cca*$^-$ in order to give the specific complex. Water cluster models and a combination of cluster and continuum solvation approaches are used

$$[Ln(H_2O)_6]^{3+}(g/s) + [cca\cdot 3H_2O]^-(g/s) \rightarrow [Ln(cca\cdot H_2O)(H_2O)_4]^{2+}(g/s) + (H_2O)_4(g/s) \quad (2)$$

$$[Ln(H_2O)_6]^{3+}(g/s) + 2[cca\cdot 3H_2O]^-(g/s) \rightarrow [Ln(cca\cdot H_2O)_2(H_2O)_2]^{+}(g/s) + 2(H_2O)_4(g/s) \quad (3)$$

$$[Ln(H_2O)_6]^{3+}(g/s) + [cca\cdot 3H_2O]^-(g/s) + 2[Cl(H_2O)_6]^-(g/s) \rightarrow Ln(cca\cdot H_2O)(H_2O)_2Cl_2(g/s) + 3(H_2O)_6(g/s) \quad (4)$$

$$[Ln(H_2O)_6]^{3+}(g/s) + 2[cca\cdot 3H_2O]^-(g/s) + [Cl(H_2O)_6]^-(g/s) \rightarrow Ln(cca\cdot H_2O)_2(H_2O)_2Cl(g/s) + 2(H_2O)_6(g/s) + (H_2O)_2(g/s) \quad (5)$$

$$[Ln(H_2O)_6]^{3+}(g/s) + 3[cca\cdot 3H_2O]^-(g/s) \rightarrow Ln(cca\cdot H_2O)_3 + 2(H_2O)_6(g/s) \quad (6)$$

A Tb(*cca*)$_2(H_2O)Cl$ composition has been suggested,[19] and for that reason the ΔE_f of a hexacoordinated Tb complex was also calculated as follows

$$[Tb(H_2O)_6]^{3+}(g/s) + 2[cca\cdot 3H_2O]^-(g/s) + [Cl(H_2O)_6]^-(g/s) \rightarrow Tb(cca\cdot H_2O)_2(H_2O)Cl(g/s) + 2(H_2O)_6(g/s) + (H_2O)_3(g/s) \quad (7)$$

In addition, ΔE_f of the Tb$(cca\cdot H_2O)_2(H_2O)(NO_3)$ complex with NO_3^- instead of Cl^- was calculated according to the following reaction scheme

$$[Tb(H_2O)_6]^{3+}(g/s) + 2[cca\cdot 3H_2O]^-(g/s) + [NO_3(H_2O)_3]^-(g/s) \rightarrow Tb(cca\cdot H_2O)_2(H_2O)(NO_3)(g/s) + 2(H_2O)_6(g/s) \quad (8)$$

Reactions 2, 3, and 6 refer to situations where no counterion is involved, whereas the remaining schemes contain either Cl^- or NO_3^- instead. The Ln^{3+} ion solvated with six water molecules, $[Ln(H_2O)_6]^{3+}$, is the reactant in eqs 2−8. The *cca*$^-$ reactant is solvated with three-water molecules ((*cca*·3H_2O)$^-$ cluster) where a water molecule is H bonded to each of the O_3, O_1, and O_6 atoms (Figure 1). The structure is stabilized additionally by two hydrogen bonds between the water molecules. In the complexes, (*cca*·H_2O) contains one water molecule hydrogen bonded to the free carboxylic oxygen of the ligand.

The formation energies presented in Table 3 characterize the stabilities of the Ln(III)−*cca* complexes. The cluster calculations showed that the stability increases with an increase of *cca*$^-$ ligands: Ln(*cca*)$(H_2O)_2Cl_2$ < Ln(*cca*)$_2(H_2O)_2Cl$ < Ln(*cca*)$_3$. The cluster approach alone provides a strong overestimation of the formation energy as compared to the combined cluster/continuum solvation calculations. Thus, the cluster models alone are not sufficient to describe the formation energy in solution reliably, and the results from the combined cluster and continuum calculations will be further discussed. The calculated formation energies in solution of the $[Ln(cca\cdot H_2O)(H_2O)_4]^{2+}$, $[Ln(cca\cdot H_2O)_2(H_2O)_2]^{+}$, and Ln$(cca\cdot H_2O)_3$ complexes without counterion (see reactions 2, 3, and 6) indicate that the stability increases with an increase of the *cca*$^-$ number. The same trend of stability in solution was found for the ionic complexes (Tb(*cca*)$^{2+}$ < Tb(*cca*)$_2^+$) on the basis of the formation constants evaluated from spectrophotometric studies.[19] The series of ΔE_f values for the neutral complexes show an ordering in stability in solution as follows: Ln(*cca*)$(H_2O)_2Cl_2$ < Ln(*cca*)$_3$ ≈ Ln(*cca*)$_2(H_2O)_2Cl$.

Implications for Luminescence Properties. The calculations on Ln(*cca*)$(H_2O)_2Cl_2$ and Ln(*cca*)$_2(H_2O)_2Cl$ complexes

Table 4. Natural Charges of the cca^- Ligand and Its Eu(III) and Tb(III) Complexes at the DFT/B3LYP/B1 Level, and Charge Decomposition Analysis (CDA) Calculated at the DFT/B3LYP/SVP Level

	natural charge				CDA	
system	Ln(III)	O_1	O_6	Cl	bond	L → Ln(III)[a]
cca^-		−0.74	−0.57			
Eu(III)	3.00					
Eu(*cca*)$^{2+}$	2.68	−1.13	−1.01		Eu−*cca*	0.895
Eu(*cca*)$_2^+$	2.73	−1.07	−0.94		Eu−*cca*	0.808
		−1.07	−0.94			
Eu(*cca*)$(H_2O)_2Cl_2$	2.56	−1.02	−0.85	−0.85	Eu−*cca*	0.693
				−0.84	Eu−H_2O	0.304
					Eu−Cl	0.793
Eu(*cca*)$_2(H_2O)_2Cl$	2.64	−1.04	−0.82	−0.86	Eu−*cca*	0.671
		−1.05	−0.84		Eu−H_2O	0.324
					Eu−Cl	0.799
Eu(*cca*)$_3$	2.88	−1.04	−0.84		Eu−*cca*	0.691
		−1.00	−0.84			
		−1.04	−0.83			
Tb(III)	3.00					
Tb(*cca*)$^{2+}$	2.67	−1.13	−1.02		Tb−*cca*	0.898
Tb(*cca*)$_2^+$	2.78	−1.11	−0.96		Tb−*cca*	0.813
		−1.11	−0.96			
Tb(*cca*)$(H_2O)_2Cl_2$	2.72	−1.04	−0.87	−0.83	Tb−*cca*	0.701
				−0.88	Tb−H_2O	0.311
					Tb−Cl	0.799
Tb(*cca*)$_2(H_2O)_2Cl$	2.81	−1.06	−0.85	−0.90	Tb−*cca*	0.668
		−1.07	−0.83		Tb−H_2O	0.326
					Tb−Cl	0.801

[a] Donation L → Ln(III).

indicate that the stability in solution, evaluated by formation energy, increases in that order. On the other hand, Ln(III)−cca^- bonding per ligand (calculated through bond lengths, ligand ΔE_{def}, and ΔE_b values) in the gas phase as well as in solution shows stronger interactions in Ln(*cca*)$(H_2O)_2Cl_2$ than in Ln(*cca*)$_2(H_2O)_2Cl$. Two factors could be important for an improvement of the lanthanide cation luminescence: the stronger Ln(III)−cca^- bonding and the adduct stability. It is believed that the first factor plays a crucial role for efficient ligand−Ln(III) energy transfer and the second factor is connected to the Ln(III) protection from the solvent.[19] The lanthanide luminescence, experimentally observed in the complexes studied, increases from Ln(*cca*)$_2(H_2O)_2Cl$ to Ln(*cca*)$(H_2O)_2Cl_2$.[19] The luminescent properties could be related to the stronger Ln(III)−cca^- bonding found in that order. Even though Ln(*cca*)$_2(H_2O)_2Cl$ appears to be the more stable complex in terms of the formation energy (see Table 3, solution data), the specific stronger interactions (indicator bond lengths in solution) of Ln(III)−O_w and Ln(III)−Cl in Ln(*cca*)$(H_2O)_2Cl_2$ probably also play an important role for improving Ln(III) the luminescent yield, protecting the Ln(III) ion better from the solvent.

The discrepancy found between the shorter Ln−O_1/O_6 distances and the weaker Ln(III)−cca^- binding energy of Ln(*cca*)$_3$ as compared to those of Ln(*cca*)$_2(H_2O)_2Cl$ suggests that a specific contribution to the binding energy (not the total ΔE_b) will be more important for an effective Ln(III)−cca^- energy transfer. For that reason further analysis in terms of the energy contribution will be discussed. The emission spectrum of Ln(*cca*)$_3$ revealed that the specificity of the complex luminescence has shifted completely to Ln(III) since no ligand luminescence is found at all.[20]

Analysis of the Ln−*cca* Bonding Character. The atomic natural charges on Ln(III), O_1, O_6, and Cl in the complexes studied and the donation contribution L → Ln(III) are collected in Table 4. The calculated charges of Eu(III) and Tb(III) vary between 2.64 and 2.88 *e*; and hence, the Ln(III)−*cca* bond appears to be strongly ionic. For the complexes of series B, larger charges were found for Tb(III) as compared to those of Eu(III). The larger charges for Tb(III) are in line with the slightly larger Tb(III)−cca^- binding energies (see Table 3, absolute values) in comparison to the Eu(III)−cca^- values.

A survey of Table 4 shows that the natural charge of Ln(III) for series A increases in the order Ln(*cca*)$^{2+}$, Ln(*cca*)$_2^+$, and Ln(*cca*)$_3$. Obviously, with an increase of the number of cca^- ligands in the Ln(III) complexes the interligand repulsion increases and hence the Ln(III)−*cca* bond lengths increase. As a result, the amount of donated electron density cca^- → Ln(III) decreases and the Ln(III) charge increases. The decrease of donated charge is in line with the decrease of the Ln(III)−cca^- binding energy (per ligand) for this series of complexes, indicating that the donor−acceptor contribution is important in addition to the ionic interaction. The same relation between natural charge of Ln(III) complexes and Ln(III)−cca^- binding energy per ligand is observed in series B.

The CDA method gives the possibility of estimating the donation contribution of each ligand to the metal ion, Table 4. CDA analysis shows a somewhat larger cca^- → Eu(III) donation for the Eu(*cca*)$(H_2O)_2Cl_2$ and Eu(*cca*)$_3$ complexes as compared to that of Eu(*cca*)$_2(H_2O)_2Cl$, Table 4. CDA values for the Ln(III)−H_2O pair are significantly smaller than the values for the pairs Ln(III)−cca^- and Ln(III)−Cl^- involving the negatively charged ligands.

On inspecting the natural charges of Table 4, increased negative charges are observed on the O_1 and O_6 atoms with respect to the free cca^- ligand, which corresponds to a strengthening of the Ln−O_1 and Ln−O_6 bonds and an increasing $\delta^-\,\delta^+$ polarization of the O_1−C and O_6=C bonds. The negative charge on the O_1 atom increases by 0.27−0.4 *e* upon complexation, while the charge on O_6 increases by 0.27−0.55 *e*. It is interesting to note that in the Ln(*cca*)$^{2+}$ and Ln(*cca*)$_2^+$ complexes a larger increase of the negative

Table 5. Binding Energy La(III)−cca^- (in kcal/mol), Energy Partitioning Analysis (EPA) of La(III)−cca^- Bonding, and Natural Charge of La(III)

	B3LYP/B1	EPA PW91/TZP				charge
system	ΔE_b[a]	ΔE_b[a,b]	ΔE_{elstat}	ΔE_{orb}	ΔE_{Pauli}	La(III)
La(*cca*)$(H_2O)_2Cl_2$	−195.1	−188.0	−188.1	−79.0	79.0	2.55
La(*cca*)$_2(H_2O)_2Cl$	−171.4[av,c]	−167.4[av]	−168.4[av]	−74.4[av]	75.4[av]	2.62
La(*cca*)$_3$	−164.1[av]	−162.0[av]	−159.7[av]	−78.1[av]	75.9[av]	2.68

[a] $\Delta E_b = E_{complex} - E(cca^-) - E(LaX^+)$ (X denotes the remaining ligands). [b] $\Delta E_b = \Delta E_{elstat} + \Delta E_{Pauli} + \Delta E_{orb.}$ [c] av = average values of ΔE.

charge is observed on O_6, while in Ln(*cca*)$(H_2O)_2Cl_2$ and Ln$(cca)_2(H_2O)_2$Cl both O atoms show similar charge increases (by ~0.3 *e*) relative to the free cca^- ligand. The bonding orbital polarizations calculated in terms of the natural bonding orbital analysis indicated that upon complexation the $C-O_6$ bond is less polarized in comparison with the $C-O_1$ bond.[21] Hence, it had been suggested that the charge transfer to Ln(III) comes mainly from the O_1 atom. This means that for the efficient cca^-−Ln(III) energy transfer the $Ln-O_1$ bond is more important than $Ln-O_6$.

In order to provide further insight into the Ln(III)−cca^- bonding situation the EPA scheme was used for the decomposition of bond energies.[52,53] The electrostatic energy (ΔE_{elstat}) is used to estimate the strength of the electrostatic bonding, and the orbital energy (ΔE_{orb}) can be associated with the covalent contributions to the bond. To avoid the problem with the open-shell systems of Sm(III), Eu(III), and Tb(III), the EPA analysis was performed for the La(III) complexes in the series La(*cca*)$(H_2O)_2Cl_2$, La$(cca)_2(H_2O)_2$-Cl, and La$(cca)_3$. As can be seen from Table 5, B3LYP and PW91 binding energies agree well. The La(III)−cca^- binding energies, ΔE_b, show the same trend for the Sm(III), Eu(III), and Tb(III) complexes discussed above (Table 3). The La-(III)−cca^- bonding situation is described using charged closed-shell fragments: (1) cca^- and (2) $[La(H_2O)_2Cl_2]^+$, $[La(cca)(H_2O)_2Cl]^+$, or $[La(cca)_2]^+$, respectively, as bonding partners. Generally, the electrostatic attractions between the charged fragments follow the trend of the binding energies and decrease in the order La(*cca*)$(H_2O)_2Cl_2$ > La$(cca)_2$-$(H_2O)_2$Cl > La$(cca)_3$. Note, the decrease in the total binding energy ΔE_b above is not in line with the increasing La(III) charges, Table 5. The smaller charges in La(*cca*)$(H_2O)_2Cl_2$ and La$(cca)_2(H_2O)_2$Cl complexes as compared to La$(cca)_3$ can be explained by electron donation from Cl^- and H_2O to La(III). Therefore, the metal charge is not an indicative measure for the attraction within the Ln(III)−cca^- bonding in the Ln(III) complexes.

The ratio $\Delta E_{elstat}/\Delta E_{orb}$ shows that the La(III)−cca^- bonds have more electrostatic than covalent character. Nevertheless, covalent interactions are important and of great interest since they play a crucial role for the effective energy transfer in the Ln(III)−cca^- complexes.[65] In this respect it is interesting to note that larger orbital interaction contributions to the La-(III)−cca^- bond were obtained for La(*cca*)$(H_2O)_2Cl_2$ and La-$(cca)_3$ than that for La$(cca)_2(H_2O)_2$Cl. As described above, an analogous order has been found for $Ln-O_1/O_6$ bond lengths and CDA values. The luminescence specificity of Ln(III) complexes, however, could be discussed in depth on the basis of excited-state calculations of these complexes.

Conclusions

The interaction of Sm(III), Eu(III), and Tb(III) with the coumarin-3-carboxylic acid was studied using DFT and supporting MP2 and CCSD(T) methods. Parallel to the decrease of the lanthanide ionic radii in the order Sm(III), Eu(III), and Tb(III), the Ln(III)−O distances in series A complexes were found to shorten and the Ln(III)−cca^- bonding interactions to strengthen. The increase of the cca^- number in the series Ln$(cca)^{2+}$, Ln$(cca)_2^+$, and Ln$(cca)_3$ complexes leads to the following trends: (1) elongation of Ln−O bonds due to interligand repulsion, (2) a decrease of the Ln(III)−cca^- bonding strength per ligand, and (3) an increase of the Ln(III) charge and a decrease of the covalent contribution to the Ln(III)−cca^- interaction.

Series B, in which the first coordination shell of the Ln-(III) cation includes additional counterions and water molecules, has been designed to give a more realistic representation of the bonding situation in solution. It is found that inclusion of specific interactions in the first solvation sphere and continuum solvation is necessary in order to produce a balanced description of structural and energetic data. In our attempts to analyze the Ln(III)−L bonding situation, great care has to be taken to distinguish between global quantities such as formation energies and specific bonding parameters, which have been deduced from model analysis. In the former case many factors such as Ln(III)−cca^- bonding and also counterions and directly bonded water molecules will contribute, producing a quite complex picture. On the other hand, it has been found that for the characterization of the Ln(III)−cca^- bond the various decomposition methods can be employed successfully. Analysis of all bonding contributions led to the expected picture of a dominant electrostatic interaction, i.e., a strongly ionic Ln(III)−cca^- bond, and revealed variations of the orbital interaction term (covalent contributions) in the 1:1, 1:2, and 1:3 Ln(III)−cca^- complexes. The latter contributions were of special interest for assessment of the luminescence properties of the Ln(III)−cca^- complexes. The experimentally observed decrease in total quantum yield of Ln(III) between the 1:1 and 1:2 Ln-(III)−cca^- complexes correlates well with computed Ln−O bond distances (gas phase and solution), Ln(III)−cca^- binding energies, ligand deformation energies, and Ln(III)−cca^- orbital interaction energies. The remarkable experimental observation of complete concentration of the luminescence specificity into the Ln(III) ion for the (1:3) complexes can in principle also be traced back in our results. The energy decomposition calculations of the 1:2 and 1:3 complexes showed that the orbital interaction terms (covalent contributions) do not follow the total binding energy order. In going from 1:2 to 1:3 the somewhat shorter Ln(III)−cca^- bond lengths and the larger orbital interaction energy can be related to the luminescent specificity of 1:3 complex. This finding suggests that these specific bonding characteristics in the ground state are probably important for the photophysical properties and luminescence specificity of the Ln-(III) complexes. However, the computed changes in the Ln(III)−cca^- bond parameters are not sufficiently pronounced in order to explain these specificities based on the ground-state data alone. For an in-depth discussion of this topic an investigation of excited-state properties of these complexes will certainly be required. Corresponding investigations on electronically excited Ln complexes are planned in our group for the near future.

(65) Faustino, W. M.; Malta, O. L.; Teotonio, E. E. S.; Brito, H. F.; Simas, A. M.; de Sá, G. F. *J. Phys. Chem. A* **2006**, *110*, 2510.

Acknowledgment. I.G. acknowledges financial support by the Austrian Academy of Sciences during her stay at the Institute for Theoretical Chemistry, University of Vienna, in the framework of the Bilateral Exchange Agreement Austria−Bulgaria. We thank Professor Peter Schuster for his support of this work. This work was supported by the Austrian Science Fund within the framework of the Special Research Program F16 (Advanced Light Sources) and Project P18411-N19. The calculations were performed in part on the Schrödinger III cluster of the University of Vienna.

Supporting Information Available: Cartesian coordinates of the investigated compounds and model structures. This material is available free of charge via the Internet at http://pubs.acs.org.

IC7016616